Carbohydrate Polymers **21** (1993) 91-95

Structural features of fatty acid–amylose complexes

M.C. Godet, A. Buléon, V. Tran & P. Colonna

Institut National de la Recherche Agronomique, BP 527, 44026 Nantes Cedex, France

X-ray diffraction and Differential Scanning Calorimetry measurements were performed on highly crystalline complexes prepared from amyloses and fatty acids with different chain lengths. The complexes yielded very sharp V_h-type diffraction diagrams except those prepared with the shortest amylose chains. The melting temperature of the complexes increased with increasing amylose chain length. In parallel, the inclusion of the fatty acid inside a 6_5 amylose helix, similar to that determined for the V_h structure, was studied using molecular modelling. The aliphatic part of the fatty acid can be included in *trans* conformation. Six discrete positions per helix pitch were calculated. The polar group of the fatty acid cannot be included, due to both steric and electrostatic repulsions.

INTRODUCTION

Amylose, the linear starch polysaccharide, crystallizes in different polymorphic forms depending on the conditions of crystallization (Buléon *et al.*, 1984). Three main crystalline allomorphs A, B and V are well documented (Sarko & Zugenmaier, 1980). In A and B crystals, also present in native starches, the chains are intertwined in double helices (Wu & Sarko, 1978*a*, *b*; Imberty & Perez, 1988; Imberty *et al.*, 1988). V amylose is a generic name for crystalline amyloses obtained as single helices co-crystallized with compounds such as water, iodine, DMSO, alcohols or fatty acids. Some of these structures (V_A, V_H, V_{DMSO}, V_{IODINE}) have been precisely characterized by X-ray analysis of crystalline fibres (Winter & Sarko, 1974; Zugenmaier & Sarko, 1976; Bluhm & Zugenmaier, 1981; Rappenecker & Zugenmaier, 1981) or from electron diffraction data (Brisson *et al.*, 1991). The chain conformation consists in a left-handed six residue 6_5 helix with a rise of between 1·32 and 1·36 nm per monomer. For V_{DMSO} and V_{IODINE} complexes (Winter & Sarko, 1974; Bluhm & Zugenmaier, 1981), the central cavity inside the single helix is occupied by two DMSO and approximately three iodine molecules per turn.

The structure of fatty acid–amylose complexes is not completely elucidated. Several models have been proposed for the inclusion of fatty acid in a V_H type amylose helix (Carlson *et al.*, 1979; Jane & Robyt, 1984; Biliaderis & Galloway, 1989) from X-ray diffraction (Mikus *et al.*, 1946), N.M.R. (Bulpin *et al.*, 1982) and Raman (Carlson *et al.*, 1979) measurements. But no precise crystallographic structures are available since it has not been possible up to now to prepare crystalline fibers or single crystals suitable for X-ray or electron diffraction.

The goal of this study was to clarify the structure and the mechanisms of formation of the fatty acid–amylose complexes. X-ray diffraction and Differential Scanning Calorimetry (DSC) characterizations of highly crystalline complexes, obtained from amylose and fatty acids with different chain lengths, were carried out in parallel with the molecular modelling of the fatty acid inclusion inside the amylose helix.

MATERIALS AND METHODS

Materials

Amylose fractions (DP 20 and 30) were obtained by mild acid hydrolysis of potato and wrinkled pea starches respectively. DP 40 was prepared by enzymatic hydrolysis of amylose gels. DP100 amylose was

*To whom correspondence should be addressed.

Carbohydrate Polymers 0144-8617/93/$06.00

supplied by Hayashibara Biochemical laboratories and DP900 amylose by Avebe (Avebeweg, Netherlands). Caprylic (C_8), lauric (C_{12}) and palmitic (C_{16}) acids were obtained from Sigma chemical Company (St Louis, MI, USA).

Crystallization

Amylose solution (0·6 g in 10 ml) and fatty acid solution (60 mg in 1 ml) in Me2SO were mixed at 90°C. Water (25 ml) was added at precipitant at 90°C. The mixture was then allowed to cool down to 25°C (cooling rate 5°C h^{-1}). The crystalline suspension was then washed by centrifugation in a 50/50 (v/v) ethanol-water mixture and stored at a water activity aw = 0·75.

X-ray diffraction

Diffraction diagrams were recorded using a Inel X-ray generator operating at 40 KV and 30 mA and a curve position sensitive detector (Inel CPS120). $CuK_{\alpha 1}$ radiation (0·15405 nm) was selected using a quartz monochromator. The samples (100 mg dry matter) were sealed between two aluminium foils to prevent any significant change in the water content during the measurement.

Differential Scanning Calorimetry

DSC measurements were carried out using a Setaram DSC111 device. Samples (25 mg) and water (85 mg) were accurately weighed into steel pans and sealed. A reference pan containing 110 mg water was used for analysis over a temperature range (30–150°C) at a heating rate of 3°C min^{-1}.

Molecular modelling

In the model usually proposed for amylose-lipid complexes (Carlson *et al.*, 1979), the aliphatic part of the lipid is inside the helical cavity of amylose. The modelling of this inclusion was carried out in two steps. In a first step, a systematic docking of a C_{12} fatty acid molecule was performed with the carboxylic group near the helix entry using a procedure derived from that of Tran *et al.* (In press) for cyclodextrin complexes. In a second step, the relative roles of the aliphatic part and the carboxylic group were studied separately. As the results of the first step showed that amylose and fatty acid axes had to be superimposed for inclusion, the positions of the aliphatic part were determined from an energy map based on the translation and the rotation along the helix axis. The low energy conformations of the carboxylic group with regard to the aliphatic chain were then determined by systematic conformational research around the two bonds C_2–C_1 and C_1–O (Fig. 1). The final solutions (i.e. inclusion of the entire fatty acid) were obtained by progressive insertion of the fatty acid, with the carboxylic group in the low-energy conformations previously calculated, following the translation/rotation map determined for the aliphatic part positions. Calculations and graphics representations were carried out with the programs INSIGHT and DISCOVER from the BIOSYM (San Diego, USA) molecular modelling package.

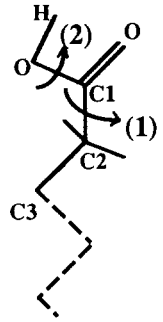

Fig. 1. Dihedrals used in the systematic search of conformations for the carboxylic group of the fatty acid.

RESULTS

X-ray diffraction

X-ray diffraction diagrams were typical of the V_h form of amylose with 3 main reflexions corresponding to Bragg angles 2θ = 7°, 13·3° and 19·8° (Fig. 2). The intensity and the sharpness of the peaks were very high except for crystals obtained from DP20 amylose. The most crystalline sample was the DP 40 amylose-palmitic acid complex.

Calorimetry

DSC thermograms contained one endotherm at about 105–115°C (Fig. 3), except for the DP30 amylose-

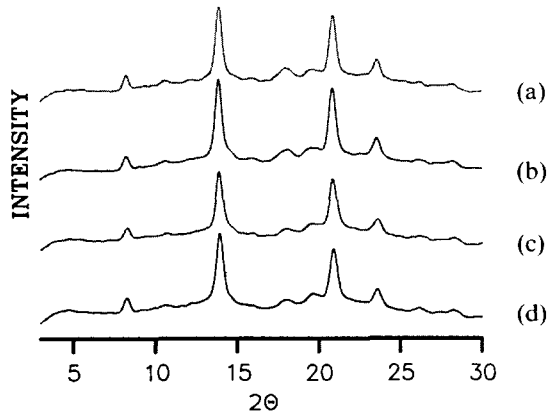

Fig. 2. X-ray diffraction diagrams of amylose-caprylic acid complexes as a function of the degree of polymerization of amylose. (a), DP30; (b), DP40; (c), DP100; (d), DP2020.

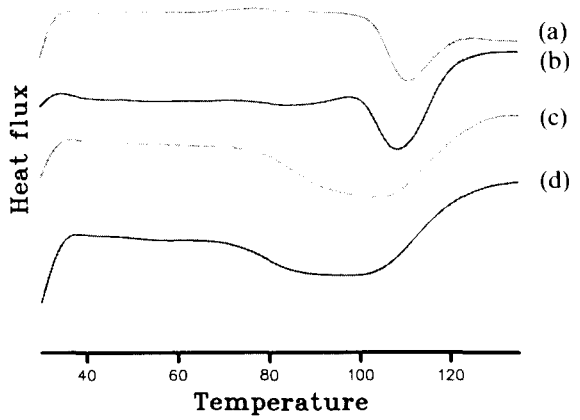

Fig. 3. Differential Scanning Calorimetry thermograms of amylose-lauric acid complexes as a function of the degree of polymerization of amylose. (a), DP2020; (b), DP100; (c), DP40; (d), DP30.

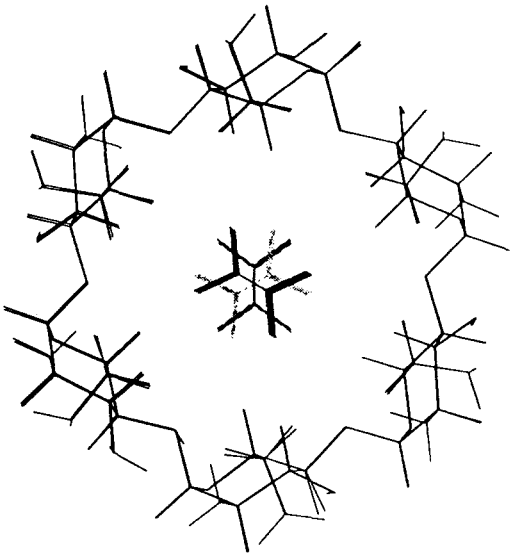

Fig. 4. Representation of the six orientations determined for the aliphatic part of the fatty acid inside the helix cavity. This view is obtained perpendicular to the helix axis.

palmitic acid complex. The melting temperatures and corresponding enthalpies are shown in Table 1. The melting temperatures increased with increasing amylose chain lengths. The crystals obtained with highest amylose and fatty acid chain lengths were the most thermostable. The enthalpies of melting decreased with decreasing fatty acid chain length. The maximum enthalpy was measured for the DP 40 amylose-palmitic acid complex.

Molecular modelling

Global docking of fatty acid inside a Vh-type helix

The inclusion of the fatty acid aliphatic chain inside the amylose helix was only possible when the aliphatic chain and the helix axes were superimposed and when the aliphatic chain was in a *trans* conformation. Six orientations (each separated by 60°) were observed for the orientations of the aliphatic carbons (Fig. 4).

Respective contributions of the two moieties of the fatty acid

The energy map calculated from rotation and translation of the aliphatic chain inside the cavity is shown in Fig. 5. There was no continuity between the low-energy solutions. The corresponding low-energy structures can be deduced by a 60° rotation and a 0·13 nm translation. The analysis of all short distances showed that only the hydrogen atoms linked to the C5 atoms of the glucopyranose residues are involved in short Van der Waals contacts with the two hydrogen atoms linked to each carbon atom of the aliphatic chain.

Four low energy conformations of the carboxylic group were calculated by systematic rotation around the C_2-C_1 and C_1-O bonds (Fig. 1). The corresponding dihedrals {C_3-C_2-C_3-O} and {C_2-C_1-O-H} were (−80,0); (−80,180); (100,0); (100,180). After insertion of the total fatty acid with the carboxylic group in these four conformations and refinement, two stable conformations were determined (Fig. 6) for the complex. For both stable solutions, the polar group was located near the entrance of the helix cavity. Further insertion of the fatty acid led to steric conflicts. Steric and electrostatic repulsions prohibited the polar group from entering the cavity.

Table 1. Melting temperatures (°C) for the amylase-fatty acid complexes as a function of amylose and fatty acid chain lengths

	DP 2020	DP 100	DP 40	DP 30
Palmitic acid (C16)	115 (24·6)	109·5 (28·1)	105 (33·3)	78·5 109 (10·3) (2·9)
Lauric acid (C12)	113·5 (16·3)	108 (26·3)	106·5 (28·0)	106 (25·5)
Caprylic acid (C8)		107·5 (20·8)	112·5 (27·0)	109 (30·4)

Corresponding enthalpies (J g^{-1} dry matter) are in brackets.

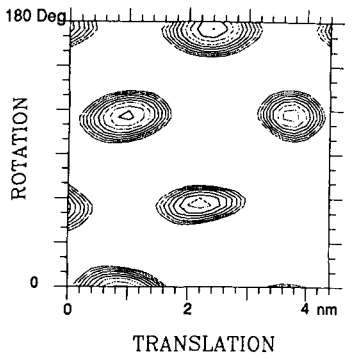

Fig. 5. Energy map calculated from relative translation and rotation of the aliphatic part of the fatty acid inside the helix cavity.

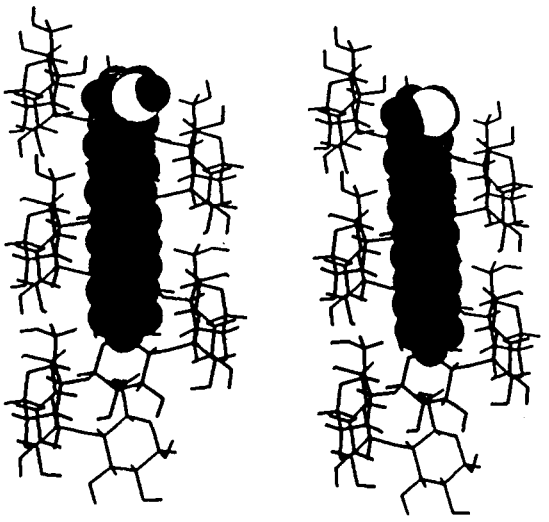

Fig. 6. Final low-energy conformations proposed for the amylose-fatty acid complex.

DISCUSSION

All obtained X-ray powder diffraction diagrams are characteristic of the V_h-type of amylose. The structure of this polymorph has been carefully determined from crystallographic analysis on crystalline fibres (Zugenmaier & Sarko; Rappenecker & Zugenmaier, 1981) and from electron diffraction data (Brisson *et al.*, 1991). In any case, the chain conformation consists of a left-handed six residue 6_5 helix amylose complexes, two hypotheses can be considered: that the fatty acid chain is included inside the amylose helix and that the fatty acid chain is laying outside amylose helices in the crystal unit cell. But in both cases the presence of the fatty acid molecules must yield no distortion of the unit-cell, since pure V_h-type diffraction patterns are obtained. In this work, the first hypothesis has been checked. Other conformations for an amylose helix such as 7_1 were not considered. Such a model has been proposed by Neszmelyi *et al.* (1987) for fatty acid complexes from molecular modelling calculations. It has been also considered for other amylose complexes with branched chain alcohol, cyclohexanol or halogenated alkyl compounds (Yamashita *et al.*, 1973; Jane & Robyt, 1984) for example. Nevertheless, these helices as well as the 8_1 models proposed for other complexes (Yamashita *et al.*, 1973) need to be confirmed and established with the same precision as the well documented 6_5. The 7_1 has also been proposed for the less stable forms observed in DSC measurements with a melting endotherm at about 80°C, and which can be transformed by annealing into a classical complex crystallized at a higher temperature and melting at 100–110°C (Raphaelides & Karkalas, 1988). It could be present in the fatty acid-amylose complexes obtained with DP 30 amylose and palmitic acid which present two endotherms. Nevertheless, the presence of two endotherms has also be attributed in other cases to isolated inclusion compounds (i.e. amylose chain plus fatty acid) without any crystalline packing of these isolated complexed chains into sufficiently large crystals (Whittam *et al.*, 1989). The increasing melting temperature observed with increasing amylose chain length could be related to the crystallite size in the crystalline complexes. High DP amyloses could yield longer crystals along the c axis, as observed for the differences between amylose and amylopectin gels (Ring *et al.*, 1987). The melting enthalpies could be connected to the quality of the amylose packing in the complexes. A longer fatty acid is supposed to orient the crystallites on a longer distance. Nevertheless, there is probably an optimal amylose chain length for the lateral junctions between individual complexed amylose chains involved in the crystalline packing. The maximum enthalpy (and also crystallinity) observed for the DP40 amylose-palmitic acid complex could also be explained by the presence of two fatty acid molecules in the amylose chain (with polar groups at each helix end). Under these conditions, a minimum uncomplexed segment, with few possible distortions with regard to a perfect 6_5 helix, is present in the amylose chain. For longer amylose chains, more than two fatty acid molecules can be present and the amylose chain is probably distorted for accepting the polar groups which cannot be included, as shown by the molecular modelling results. These results show that the inclusion of the aliphatic part of the fatty acid inside the amylose helix, in a 6_5 conformation, is possible but only with discrete positions which correspond to a very tight packing. The close packing is due to the related symmetries of both the 6_5 helix and the calculated positions of aliphatic chains. This close association could be obtained only after a very mobile state for the amylose chain, i.e. a good solvent and sufficiently high temperature, which explains why the high crystalline samples are only prepared at 90°C.

REFERENCES

Biliaderis, C.G. & Galloway, G. (1989). *Carbohydr. Res.*, **189,** 31–48.

Bluhm, T.L. & Zugenmaier, P. (1981). *Carbohydr. Res.*, **9,** 1–10.

Brisson, J., Chanzy, H. & Winter, W.T. (1991). *Int. J. Biol. Macromol.*, **123,** 31.

Buléon, A., Duprat, F., Booy, F. & Chanzy, H. (1984). *Carbohydr. Polym.*, **4,** 161.

Bulpin, P.V., Welsh, E.J. & Morris, E.R. (1982). *Starke*, **34,** 335.

Carlson, T.L.-G., Larsson, K., Dinh-Nhuyen & Krog, N. (1979). *Starke*, **31,** 222.

Imberty, A. & Perez, S. (1988). *Biopolym.*, **27,** 1205.

Imberty, A., Chanzy, H., Perez, S., Buléon, A. & Tran, V. (1988). *J. Mol. Biol.*, **201,** 365.

Jane, J.-I. & Robyt, J.F. (1984). *Carbohydr. Res.*, **132,** 105–18.

Mikus, F.F., Hixon, R.M. & Rundle, R.E. (1946). *J. Am. Chem. Soc.*, **68,** 1115.

Neszmelyi, A., Laszlo, E. & Hollo, J. (1987). *Starke*, **11,** 393.

Raphaelides, S. & Karkalas, J. (1988). *Carbohydr. Res.*, **172,** 65.

Rappenecker, G. & Zugenmaier, P. (1981). *Carbohydr. Res.*, **89,** 11.

Ring, S., Colonna, P., l'Anson, K.J., Miles, M.J., Morris, V.J. & Oxford, P. (1987). *Carbohydr. Res.*, **162,** 277.

Sarko, A. & Zugenmaier, P. (1980). In *Fiber diffraction methods* eds A.D. French & K.C. Gardner. ACS symposium series, **141,** 459.

Tran, V., Delage, M.M. & Buléon, A., (In press). *J. Inclusion phenom.*

Whittam, M., Orford, P., Ring, S., Clark, S., Parker, M., Cairns, P. & Miles, M. (1989). *Int. J. Biol. Macromol.*, **11,** 339.

Winter, W.T. & Sarko, A. (1974). *Biopolym.*, **13,** 1461.

Wu, H.C. & Sarko, A. (1978*a*). *Biopolym.*, **61,** 7.

Wu, H.C. & Sarko, A. (1978*b*). *Biopolym.*, **61,** 27.

Yamashita, Y., Ryugo, J. & Monore, K. (1973). *J. Electron Microscopy*, **22,** 19.

Zugenmaier, P. & Sarko, A. (1976). *Biopolym.*, **15,** 2121–36.